

## State-Resolved Scattering of Molecules in Pendular States: ICl + Ar

B. Friedrich,<sup>(a)</sup> H.-G. Rubahn, and N. Sathyamurthy<sup>(b)</sup>

Max-Planck-Institut für Strömungsforschung, Bunsenstrasse 10, W-3400 Göttingen, Germany

(Received 23 June 1992)

The effect of pendular orientation of the figure axis of ICl on elastic and inelastic scattering by Ar was explored in a crossed beam experiment. The pendular states of ICl are created by hybridizing its rotational states up to  $J \leq 3$  in a uniform electric field of strength  $\mathcal{E} = 100$  kV/cm. The resulting change in the distribution of individual  $J$  states of ICl is measured state-selectively by laser-induced fluorescence near the zero scattering angle outside the field. We find that the electric field inhibits rotationally inelastic scattering of low- $J$  state molecules, due to a larger spacing between levels.

PACS numbers: 34.40.+n, 34.50.-s, 35.20.Bm, 82.40.Dm

Strong uniform electric or magnetic fields can hybridize low rotational states of molecules that possess an electric or magnetic moment coupled to one of the molecular axes [1,2]. This hybridization creates pendular states in which the molecular axis is confined to librate over a limited angular range about the field direction; the corresponding eigenenergies form a characteristic ladder and their eigenfunctions are directional, making the axis of molecules in pendular states inherently aligned or oriented. This provides the means to avoid the usual averaging over random orientations of colliding molecules and thereby enhance the dynamical resolution of collision experiments [3].

Direct spectroscopic demonstrations thus far have oriented polar molecules in a static electric field [4,5]. Electric pendular orientation has been applied to the study of the steric effect in reactive collisions of ICl and  $\text{CH}_3\text{I}$  with K [1]. In these experiments the molecular dipole is oriented either parallel or antiparallel to the reactant relative velocity vector and the difference in the reactivity of the heads and tails of the reagent molecules is examined.

We undertook an experimental and theoretical study to explore how both the directionality *and* the characteristic eigenenergies of pendular states affect state-to-state collisions. We orient ground-state ICl molecules by sending them into a uniform electric field of strength  $\mathcal{E} = 100$  kV/cm. Within the field, the ICl supersonic beam is crossed with an Ar beam. In this arrangement the field strength  $\mathcal{E}$  is perpendicular to the initial Ar-ICl relative velocity vector,  $k$ . The attained field strength is sufficient to hybridize the rotational states of ICl up to  $J \leq 3$  and thereby create ten pendular states. The orientation is characterized by the expectation value,  $\langle \cos\theta \rangle$ , of the angle  $\theta$  between the figure axis and the direction of the electric field. Pendular eigenproperties depend solely on the parameter  $\omega \equiv \mu\mathcal{E}/B$  which measures the electric dipole energy,  $\mu\mathcal{E}$ , in units of the rotational constant,  $B$ . Figure 1 shows the low field-free rotor  $J$  levels ( $\omega = 0$ ) together with the eigenenergies and the expectation values of the orientation cosine for the  $(J, |M|)$  pendulum or pinwheel states at  $\omega = 18.3$ ; the latter are labeled with the quantum

number  $J$  of the parent field-free rotor state and the modulus  $|M|$  of the projection of the rotational angular momentum  $J$  on the field direction.

The experimental setup is shown schematically in Fig. 2. The molecular beam containing about 20% of ICl seeded in Ar is formed by expanding the gas mixture at 50 torr and 310 K through a glass nozzle 300  $\mu\text{m}$  in diameter. The beam is collimated by a skimmer 2 mm in diameter and sent into the differentially pumped scattering and observation chamber. There the beam passes between two planar 2 cm  $\times$  2 cm electrodes 1 mm apart, fashioned from polished stainless steel. A secondary Ar

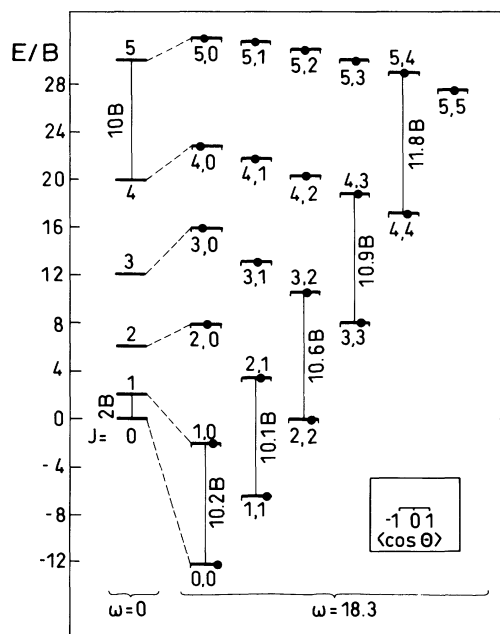


FIG. 1. Energy levels and orientation of ICl. Left: field-free rotational levels labeled with  $J$  ( $\omega = 0$ ). Right: pendular levels labeled with  $J, |M|$  for  $\omega = 18.3$ ; position of dot on each level indicates the expectation value of the orientation cosine,  $\langle \cos\theta \rangle$ . The given value of  $\omega$  obtains for the dipole moment  $\mu = 1.24$  D and the rotational constant  $B = 0.114156$   $\text{cm}^{-1}$  of  $\text{ICl}(X^1\Sigma_0, v'' = 0)$  at  $\mathcal{E} = 100$  kV/cm [6].

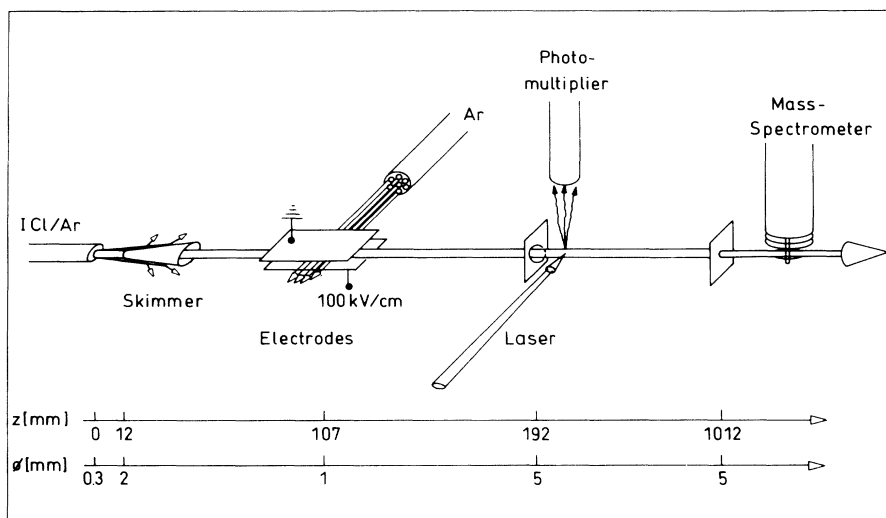


FIG. 2. Experimental setup. The supersonic beam of ICl seeded in Ar is passed between two planar electrodes where it is crossed by a secondary Ar beam. The rotational distribution of ICl is probed by LIF outside the field. A mass spectrometer measures attenuation of the ICl signal. Distances,  $z$ , from the nozzle and diameters,  $\Phi$ , of collimating elements are also indicated.

beam effuses from a multichannel array and attenuates the primary beam between the electrodes by 40%; the center-of-mass collision energy,  $E_{\text{coll}}$ , is 40 meV ( $323 \text{ cm}^{-1}$ ). The rotational state distribution of ICl is probed by laser-induced fluorescence (LIF) excited by a ring dye laser (Coherent CR 699-21) propagating perpendicular to the ICl beam 85 mm downstream from the scattering center. In addition, a quadrupole mass spectrometer located 820 mm downstream from the photomultiplier tube measures the ICl intensity summed over all its rotational states. The angular resolution about the zero scattering angle, as defined by the spatial confinement of the LIF and mass-spectrometric detection, is  $3.4^\circ$  and  $0.32^\circ$ , respectively.

The rotational transitions were measured within the  $A^3\Pi_1 \rightarrow X^1\Sigma_0$  ( $v'=19, J' \rightarrow v''=0, J''$ ) vibronic band and their hyperfine structure was clearly resolved (linewidth 25 MHz). The rotational states  $J''$  of the vibronic ground-state manifold were assigned in agreement with Ref. [6]. The fluorescence intensities were used to determine the rotational state distribution of ICl resulting from the beam expansion, cf. Table I; the fluorescence intensities for a given  $J$  were obtained by summing up contributions from the respective hyperfine components.

When the secondary Ar beam is absent, the appearance of the spectrum outside the electric field is independent of the field strength. This is connected with the hybrid nature of pendular states: The coherent superposition of field-free rotor states takes place only within the field; the molecules bear no memory of their hybridization state, in accordance with Ehrenfest's adiabatic principle.

Only with the secondary beam on, the population of rotational states becomes field dependent, reflecting the changes in scattering cross sections due to pendular orientation. With the secondary beam present, we measure fluorescence intensities,  $I_J$ , arising from the excitation of various  $R_J$ ,  $Q_J$ , and  $P_J$  transitions of ICl, either with the electric field on,  $I_J(\mathcal{E})$ , or off,  $I_J(0)$ . Since no hyperfine state dependence of the cross sections was found, the fluorescence intensities for a given  $J$  state were determined by integrating over a spectral linewidth of the most intense hyperfine component.

Figure 3 shows the relative change in fluorescence intensity,  $[I_J(\mathcal{E}) - I_J(0)]/I_J(0)$ , as a function of rotational state  $J$ . The first point on the left was obtained in a mass-spectrometric measurement: It shows the ratio of signals at the mass of ICl which, due to the high angular

TABLE I. Populations of rotational states of ICl. The initial populations  $W(J_i)$  were measured without scattering gas; the final populations  $W(J_f)_0$  and  $W(J_f)_{100}$  were calculated for the scattering by Ar under field-free conditions and within the field of 100 kV/cm, respectively. Results in parentheses were corrected for the overestimates inherent to quasiclassical trajectory calculations [8] by applying the principle of microscopic reversibility.

$J$	0	1	2	3	4	5	6
$W(J_i)$	$1.00 \pm 0.10$	$1.88 \pm 0.07$	$1.77 \pm 0.01$	$1.77 \pm 0.08$	$1.77 \pm 0.07$	$1.45 \pm 0.01$	$1.70 \pm 0.01$
$W(J_f)_0$	0.82 (0.90)	1.88 (1.80)	1.85	1.83	1.73	1.51	1.61
$W(J_f)_{100}$	1.01	1.90	1.72	1.82	1.70	1.50	1.64

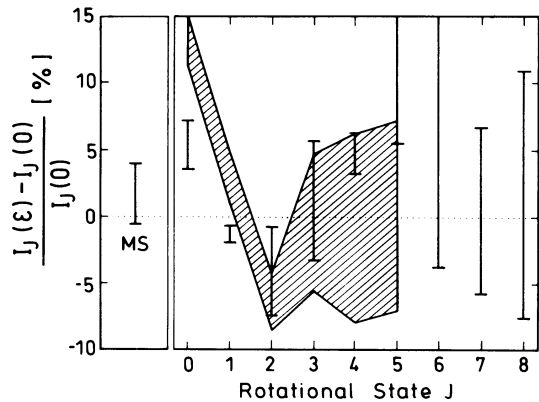


FIG. 3. Measured relative change in fluorescence intensities of ICl attenuated by Ar at field strengths of either 100 or 0 kV/cm for different  $J$  states compared with the corresponding calculated change (shaded); the scattering angle  $\Theta_{c.m.} = 0^\circ$  and the collision energy  $E_{coll} = 40$  meV. The point marked as MS was obtained in a different, mass spectrometric measurement; see text. The error bars and the widths of the shaded region represent twice the standard deviation.

resolution, is a sensitive measure of the change in total elastic cross section due to pendular orientation. Within the error bars, we observe no change in elastic scattering; this is consistent with the fact that, for a geometry with  $\mathbf{k} \perp \mathcal{E}$ , the incoming Ar atoms cannot distinguish between the heads and tails of the ICl molecules. On the other hand, the state-resolved data exhibit a significant  $J$  dependence of the relative fluorescence intensity with an oscillatory structure. For  $J \geq 5$  the changes become insignificant.

In order to explain the experimental data we carried out quasiclassical trajectory calculations. The Ar-ICl interaction was modeled by a pairwise additive (12,6) Lennard-Jones potential with  $\epsilon_{I-Ar} = 0.0140$  eV,  $\sigma_{I-Ar} = 7.090$  a.u. and  $\epsilon_{Cl-Ar} = 0.0103$  eV,  $\sigma_{Cl-Ar} = 6.435$  a.u. The ICl molecule was treated as rigid with an equilibrium bond distance of 4.3855 a.u. [7].

The  $^{127}\text{I}^{35}\text{Cl} + ^{40}\text{Ar}$  collisions were simulated by solving Hamilton's equations using the fourth-order Runge-Kutta method with a step size of 5.387 fs. The trajectories were started at an ICl-Ar center-of-mass separation of 20 a.u. and at a collision energy  $E_{coll} = 40$  meV.

Test runs were made by varying the impact parameter  $b$  at intervals of 1.0 a.u. It was found that practically all inelastic scattering processes leading to center-of-mass scattering angles  $\Theta_{c.m.} \leq 10^\circ$  (well within the experimentally detected range) take place at values of  $b$  between 13.5 and 15.5 a.u. Subsequently, the trajectories were computed by appropriate sampling of  $b$  just in this interval.

(i) *Field-free scattering.*  $10^3$  trajectories were computed for each of the initial free-rotor states  $J_i = 0, 1, \dots, 8$ . The trajectories were analyzed for the final free-rotor

states,  $J_f$ , using the standard histogram procedure, and the probabilities,  $P(J_i \rightarrow J_f)$ , of the  $J_i \rightarrow J_f$  transitions were evaluated. The rotational populations of ICl before and after the field-free collisions with Ar,  $W(J_i)$  and  $W(J_f)$ , are listed in Table I. The initial populations  $W(J_i)$  were obtained from experiment (see above) while the final ones were calculated according to  $W(J_f) = \sum_{J_i} W(J_i) P(J_i \rightarrow J_f)$ , with  $J_i = 0, 1, \dots, 8$  and  $J_f = 0, 1, \dots, 8$ . There is a significant decrease in population of  $J_f = 0$  and a substantial increase of  $J_f = 2$  and 3 while  $J_f = 1$  remains nearly constant.

(ii) *Scattering in the field.* Similar calculations and analysis were carried out for collisions within the field. The energies of the field-free  $J$  states of ICl were replaced by eigenenergies of the pendular ( $J, |M|$ ) states and it was assumed that transitions occurred only between states with the same  $|M|$ . As a test case, the range of the figure axis orientation angle  $\theta$  for transitions from the (0,0) pendular ground state was restricted by the respective classical turning points within the  $V(\theta) = -\omega \cos\theta$  pendulum potential, for  $\omega = 18.3$  (cf. Fig. 1). The trajectories showed virtually no inelasticity at scattering angles up to  $10^\circ$ . This could be reproduced by a fit of the field-free transition probabilities with an exponential gap relation [8],

$$P(J_i \rightarrow J_f) \propto [(2J_f + 1)/(2J_i + 1)] \exp[-C_i |\Delta E_{if}|],$$

with  $C_i$  a constant and  $\Delta E_{if}$  the amount of energy transferred. This analytic approximation of the transition probability was then applied to transitions involving all other pendular states. To evaluate the population redistributions, the initial populations  $W(J_i)$  of each field-free rotational  $J$  manifold (degenerate  $M_i$ ) were first adiabatically transferred into the pendular states. Within each  $J$  manifold the populations were taken to be  $W(J_i)/(2J_i + 1)$  for  $M_i = 0$  and  $2W(J_i)/(2J_i + 1)$  for  $|M_i| > 0$ . The final ( $J_f, |M_f|$ )-state populations were then adiabatically transferred back to the field-free states  $J_f$  by summing up the corresponding populations in a  $J_f$  manifold over  $M_f$ . The results are included in Table I along with the relative final populations resulting from scattering without the field as a function of  $J$ . The corresponding population changes,  $[W(J_f)_{100} - W(J_f)_0]/W(J_f)_0$ , are shown as shaded areas in Fig. 3. They represent satisfactorily the experimentally observed oscillatory behavior. A second set of calculations using  $\epsilon_{Cl-Ar} = 0.0123$  eV,  $\sigma_{Cl-Ar} = 6.626$  a.u. confirmed that despite quantitative changes in the transition probabilities the trends in the population ratios for  $J = 0-3$  remained unaltered.

The results can be understood qualitatively with the help of the energy diagram in Fig. 1. Under field-free conditions, collisions induce substantial population changes among  $J = 0, 1$ , and 2. In the presence of the field, the energy levels change and the spacing between low- $(J, |M|)$  states becomes substantially larger; for in-

stance, between the (0,0) and (1,0) states it amounts to  $10.2B$ , compared with  $2B$  between  $J=0$  and 1 in the field-free case. As a result, there is very little energy transfer from or to (0,0) and the population in  $J_i=0$  remains essentially unaltered. A similar argument holds for  $J=1$  to 3. This means that in the presence of the field, collisions with Ar at 40 meV ( $E_{\text{coll}}/B \sim 3000$ ) resulting in  $\Theta_{\text{c.m.}} \leq 10^\circ$  are essentially elastic for the low- $J$  states. Therefore, the inelasticity is due to scattering of the *field-free* molecules; the measured ratios of populations for scattering with and without the field thus reflect changes due to inelastic collisions of the field-free molecules.

Our prototype scattering experiment by pendular molecules indicates that, under favorable conditions, elastic and inelastic contributions to the total collision cross section (in the forward direction) can be separated by turning on and off a strong uniform electric field in the scattering zone. This has a wide application in the study of state-to-state collisions, including chemical reactions.

We are grateful to Professor J. P. Toennies for encouragement. B.F. owes special thanks to Professor D. R. Herschbach for his enthusiasm and support. We also profited from the skillful assistance of M. Renger and M. Verbeek during the measurements. B.F. and N.S. thank the Alexander von Humboldt Foundation for a fellowship. Partial financial support was provided by the Sonderforschungsbereich 93 "Photochemistry with Lasers" of the Deutsche Forschungsgemeinschaft.

<sup>(a)</sup>On leave from Department of Chemistry, Harvard University, Cambridge, MA 02138.

<sup>(b)</sup>Permanent address: Indian Institute of Technology, Kanpur, 208016 India.

- [1] H. J. Loesch and A. Remscheid, *J. Chem. Phys.* **94**, 4779 (1990); **95**, 8194 (1991).
- [2] B. Friedrich and D. R. Herschbach, *Z. Phys. D* **18**, 153 (1991); first presented as a part of a talk entitled *Bringing Molecules to Attention: A Tribute to J. P. Toennies*, at the Max-Planck-Institut für Strömungsforschung, Göttingen, 1 June 1990; B. Friedrich, D. Pullman, and D. R. Herschbach, *J. Phys. Chem.* **95**, 8118 (1991); B. Friedrich and D. R. Herschbach, *Z. Phys. D* **24**, 25 (1992).
- [3] R. B. Bernstein, D. R. Herschbach, and R. D. Levine, *J. Phys. Chem.* **91**, 5365 (1987), and references cited therein; P. R. Brooks, *Science* **193**, 11 (1976); S. Stolte, *Nature (London)* **353**, 391 (1991).
- [4] B. Friedrich and D. R. Herschbach, *Nature (London)* **353**, 412 (1991).
- [5] P. Block, E. Bohac, and R. E. Miller, *Phys. Rev. Lett.* **68**, 1303 (1992); J.-M. Rost, J. Griffin, B. Friedrich, and D. R. Herschbach, *Phys. Rev. Lett.* **68**, 1299 (1992).
- [6] F. E. Cummings and W. J. Klemperer, *J. Chem. Phys.* **60**, 2035 (1974); S. G. Hansen, J. D. Thompson, C. M. Western, and B. J. Howard, *Mol. Phys.* **49**, 1217 (1983).
- [7] Parameters estimated from values given by H. S. Johnston, *Gas Phase Reaction Rate Theory* (The Ronald Press, New York, 1966), p. 74.
- [8] A. D. Ding and J. C. Polanyi, *Chem. Phys.* **10**, 39 (1975); J. C. Polanyi and N. Sathyamurthy, *Chem. Phys.* **29**, 9 (1978).